ORIGINAL ARTICLE
Journal Section

Improving quantitative structure models of trees inspired by pipe and metabolic scaling theory

Jan Hackenberg PhD[1*] | Jean-Daniel Bontemps HDR[2*]

[1]SimpleForest, Aachener Str. 5d, Koblenz, RlP, 56072, Germany

[2]IGN, Laboratoire d'Inventaire Forestier, 14 rue Giradet, 54000 Nancy

Correspondence
Jan Hackenberg
Email: jan.hackenberg@posteo.de

Funding information

We invent here in this manuscript new tree describing parameters which can be derived from a QSM. QSMs are topological ordered cylinder models of trees which describe the branching structure completely.

All new invented parameters have in common, that their defining point of view looks from the direction of the tips and not from the root along the tree. The reason here is simple, diameter relations are stronger when they rely on a distance measure to the tip(s) rather than on a distance measure to the root. In the traditional branch order for example different sized branches are contained, but in the reverse branch order this problem is barely exiting anymore.

The pipe model theory (PMT) is a theory adapted to deciduous trees based on the allometric scaling theory. And according to the PMT the count of new growth units can serve as a proxy to predict the sapwood area at the query cylinder's cross section. By multiplying this area proxy with the cylinder length we receive a proxy for the sapwood volume contained. We name the sapwood volume of the whole subbranch VesselVolume.

The sapwood volume finally serves as the predictor for the basic allometry function to predict the diameter/radius of combined sap and heartwood at the query point.

For validation we use QSMs produced from an open point cloud data set of tree clouds with SimpleForest soft-

ware. We compare the QSM volume against the harvested reference data for 66 felled trees. We also found QSM data of TreeQSM, a competitive and broadly accepted QSM modeling tool. Our RMSE was less than 40 % of the TreeQSM RMSE.

And for other error measures, the $r^2_{adj.}$ and the CCC, the relative improvement looked even better with reaching only 27 % and 21 % of the TreeQSM errors respectively. With the invention of this filter we improve tree volume prediction capabilities utilizing QSMs. Additionally, we run numerical tests against the West Brown Enquist (WBE) model predictions using our filtered QSMs.

KEYWORDS
Allometric Scaling, Trees, SimpleForest, QSM, Metabolic Scaling Theory, Pipe Model Theory, West, Brown and Enquist (WBE) Model

1 | INTRODUCTION

The scope of this manuscript is the invention of new tree describing parameters which have better correlation with radius/diameter measurements at any point of a tree compared to traditional tree describing parameters. We run automated methods on 3d point cloud data using those parameters to build an efficient filter for volume predictions. We use here terrestrial laser scan (TLS) data. From TLS clouds we build quantitative structure models (QSM) - topological ordered cylinder models describing the branching structure of trees (Raumonen et al., 2013; Hackenberg et al., 2014; Markku et al., 2015). On those QSMs we explore new tree modeling techniques. We wrap new methods into a context of traditional forest ecological theories.

Before we use the proposed protocol we want first look back in time to get an insight how efficient the digital method is compared to traditional analysis.

Many ways to predict the above ground volume of trees with mathematical concepts have been performed over the last centuries. Already 500 years ago Leonardo da Vinci noticed that the sum of cross sectional areas at any height equals the cross sectional area of the stem (Richter et al., 1970). From this hypothesis a Volume prediction model utilizing the Diameter at Breast Height (DBH) and the Height (H) follows, see equation 1.

$$Volume = H \times DBH^2 \times \frac{\pi}{4} \tag{1}$$

While we know this equation overestimates the Volume it is a quite fundamental ecological observation based statistical tree model because the cylinder formula is a really simple geometric form. Additionally it relies only on two easy to obtain field parameters.

Also in da Vinci's work firstly the comparison of a tree's branching system with a river network was performed.

An important ordering attribute describing river networks is the number of sources feeding that part of the river. We will discuss in this manuscript expressing branch orders in a reverse and recursive way and one of our tree parameters discussed is the pendant to that river network measure.

An important explanation for the overestimation caused by equation 1 is the lack of a component which describes the tapering of stem or branch segments. All segments, that is tree parts between two neighboring branch junctions, have the tendency to decrease their diameter if we look from closest to the root to furthest from the root along the segment.

Due to data limitations often only partial volume predictor functions fo exist in a published form. Branch volume is often ignored and we can for example only express the tree's stem volume with formulas as we can see in equation 2. The tree species specific form factor f describes the taper of the stem and is published for various species (van Laar and Akça, 2007) .

$$Volume = \frac{\pi}{4} \times DBH^2 \times H \times f \tag{2}$$

We can find those and other similar tree species specific equations in online data bases (Henry et al., 2013; Zianis et al., 2005). Nevertheless, utilizing those equations comes with a large uncertainty about the prediction accuracy, especially if regional growth pattern are accounted to. With traditional methods the `Volume` could only be destructively collected with high field costs. To retrieve a `Volume` estimate for a single tree the tree had to be felled, sawed into segments, dried and weighted. The total above ground biomass (`AGB`) is then multiplied with the density ρ.

1.1 | Allometric Theory

An interesting `Volume` predictor function for trees is the commonly used power function in equation 3.

$$Volume = a \times DBH^b \tag{3}$$

The function is interesting in the sense that it describes the total `Volume` of above ground wood components including branching structure.

Using power functions to model size relations is not limited to trees. The theory of allometric scaling relying on exactly that base function is a general biological theory, see equation 4 for the generalization.

$$Y_i = a \times X_i^b \tag{4}$$

A century ago Huxley analysed size relations on the data of shore-crab bodies and realized he could linearize the problem by a simple log transform on predictor and predicted, as we can see in equation 5 (Huxley, 1924). The error ϵ_i follows a normal distribution with mean 0 and standard deviation σ^2. Huxley assumed an homoscedastic error constant over the full range of log transformed data, see equation 5.

$$ln(Y_i) = ln(a) + b \times ln(X_i) + \epsilon_i, \epsilon_i \sim N(0, \sigma^2) \tag{5}$$

After the linear fit the back transformation to the power function shown in equation 6 was performed by Huxley.

$$Y_i = a \times X_i^b \times exp(\epsilon_i), \epsilon_i \sim N(0, \sigma^2) \tag{6}$$

However, the variation in the presented model now is a multiplier for the mean function, which means that the residuals of Y will increase as X increases. In other words, the distribution for the response variable in the model will be heteroscedastic.

The hypothesis that a part of an organism will generally grow in proportion to some constant power of the size of the whole organism was applied in other works in the following years (Medawar, 1950).

One limitation of the allometric scaling analysis protocol published by Huxley (Huxley, 1924) was that the protocol required data which had a linear pattern in the logarithmic domain. Various data sets however did not fullfill this precondition but rather had curvilinear form in the logarithmic domain. For a while such data could not be modeled with the allometric scaling theory.

Fifty years after Huxley's early work science started to apply non linear regression on allometric scaling data which was not logarithmic transformed (Zar, 1968; Glass, 1969).

Their non linear solver relied on a homoscedastic error, see equation 7.

$$Y_i = a \times X_i^b + \epsilon_i, \epsilon_i \sim N(0, \sigma^2) \tag{7}$$

This approach was received critically at the biology audience in the first decade (Bainbridge, 1969; Hafley, 1969; Lasiewski, 1969; Lasiewski and Dawson, 1969; Manaster B. J., 1975). The reasoning of the conservative reception was about the fact that the size of residuals of response Y_i typically increased substantially with the value for X_i. So a model relying on a heteroscedasticity domain error was preferred.

We get more review details on allometric scaling, its different development over the last century (Packard, 2019).

After giving an overview in the first part of the manuscript Packard then presents a well designed protocol to analyze 22 different statistical functions relying on the base equation 3. The used data consists of $\sim$ 90 individuals of the bivalve mollusk *Thracia phaseolina* (Sartori and Ball, 2009).

All functions do rely on advancements done to Huxley's work in the last century. Differences in the models are caused by different assumptions on the error distribution. In a first step Packard considers applying the original protocol, e.g. log transform the data and then perform a linear fit (Huxley, 1924) relying on equation 5.

Based on the performance of the Akaike's information criterion (AIC) (Anderson and Burnham, 2004; Anderson, 2008) received by applying both a first order polynomial and a second order polynomial fit he considers the tested data as inappropriate for this method as he concludes the better performing second order polynom reveals a curvilinear log scaled domain. So the non linear approach to fit a function is used from that decision on.

We gained now insight into allometric scaling basic concepts but want to turn our focus to trees again. In fact the generic allometric scaling concept can be applied to trees as well.

1.2 | Pipe Model Theory

Before the invention of the allometric scaling protocol Pressler proposed a new tree modeling theory for deciduous temperate species referred to as Pressler's law (Pressler and Pressler, 1865). The law states that the summed up cross

sectional areas of pipes formed in the latest growing season correlates to the annual diameter increment of the stem. This hypothesis was concluded from the fact that new leaves have to be fed with nutrients via new pipes building this diameter increment.

Combined with allometric scaling this theory was then even further optimized by accounting to inactive pipes as well in the Pipe Model Theory (PMT) (Shinozaki et al., 1964b,a). Due to thinning and self thinning pipes become inactive and build up the heartwood. The inactive pipes are located in the center of the stem and branching units. The active pipes which feed the leaves with nutrients build up the outer perimeter of the wooden structure. We can call this outer part sapwood.

Recently a well written summary about the PMT and related tree describing theories was published (Lehnebach et al., 2018). The PMT fulfills some conceptual properties:

1. Sapwood area and leaf area/mass are proportional. Here Pressler's law is echoed.
2. The area-preserving rule assumes that the conductive sapwood area of a stem at a given height is equal to the cumulative basal area of its daughter axes above that height. We can see here a reflection of the da Vinci rule.
3. The operating time of pipes is limited to the time frame of a year, the nutrient transporting pipes are renewed every year.

1.3 | West Brown and Enquist model

Various biological theories exist about the allometric exponential parameter b in equation 4. The parameter often takes the form of a quarter-power (Peters and Peters, 1983; Calder, 1984; Schmidt-Nielsen, 1984).

A specialization of the theory is the West, Brown and Enquist (WBE) model (West et al., 1997, 1999, 2000, 2009; Enquist et al., 2009). The WBE model is designed to be a generic biological model not limited to trees, but this time the data used to publish the theory was data originated in forest ecology. Namely the data already used fifty years ago in the publication of the PMT (Shinozaki et al., 1964a). The WBE model states that the annual growth in biomass scales as the 3/4 power of body mass. So the authors here fix the exponential b parameter in equation 4 to a constant value. They claim that such constants can be applied to everything, even the packaging of species in communities (Niklas, 2004).

The WBE model sees trees as branching networks that (Enquist, 2002):

1. supply the leaves contained in a fixed three-dimensional volume with nutrients
2. the energy required to perform the supply chain is minimized
3. the leaves and tips of the network are self-similar

The WBE model is up to date a really comprehensive model but it has also been contested on theoretical and empirical grounds (Banavar et al., 1999; Weibel, 2002).

1.4 | Tree data availability for allometric scaling research

We have now learned about a few relevant ecological theories. We discussed the complex data collection protocols which are time consuming and costly. But in the context of digitalization also new measurement devices have been developed and they already have been used successfully in the field of forest ecology. We mentioned LiDAR techniques and their ability to represent the surface of the environment with point clouds.

Static terrestrial LiDAR sensors provide in forest environments data which covers the surface of trees with point clouds. For the processing of Terrestrial Laser Scanning (TLS) data 3d tree reconstruction algorithms have been developed (Xu et al., 2007; Côté et al., 2011; Raumonen et al., 2013; Hackenberg et al., 2014; Lau Alvaro, 2018; Ye et al., 2019). Because of the automation level the human bias is minimized during data collection. Tree surfaces can easily be covered with multiple millions of euclidean points when TLS data are recorded.

Since around a decade various software tools to produce so called Quantitative Structure Models (QSMs) have been published (Demol et al., 2022a). QSMs consist of thousands and sometimes even ten or hundred thousands cylinders (Markku et al., 2015). With the complete branching structure being geometrically captured the `Volume` can be measured. Full automation in the modeling of the same data will lead to same QSMs not affected by the person running the computation. Data collection time is roughly in the time frame of few hours or days when collecting TLS data which covers up to multiple hectares of forest.

In addition to the geometrical description also topological information is stored inside a QSM. The order from the tree root to the branch tips is added to the geometry parameters. Figure 1 shows a real QSM of a large tree's point cloud with more than 35 thousand cylinders. And in figure 2 we draw an idealized and simplified mathematical QSM. We discuss the topological order represented by the informatics tree structure later to create new relevant tree parameters.

Licensed under copy left are the Computree (Othmani et al., 2013) plugins SimpleTree (Hackenberg et al., 2014, 2015a) and SimpleForest (Hackenberg et al., 2021). Also TreeQSM (Raumonen et al., 2013, 2015) and 3dForest (Trochta et al., 2017) are QSM producing tools which can be downloaded with their source code being free.

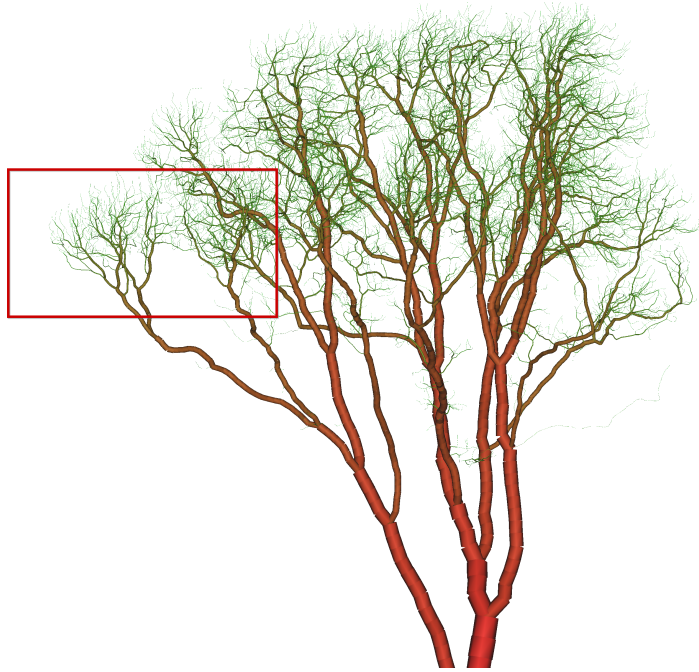

(a)

(b)

FIGURE 1

(a) A QSM of an *Acer pseudoplatanus* (Disney et al., 2018; Calders et al., 2018) with a DBH of ~ 1.4 m containing approximately 25 m^3 of woody biomass. The QSM was modeled with Simple Forest (Hackenberg et al., 2021). The tree is located in Wytham Woods, UK. The QSM consists of more than 35 000 cylinders.
(b) An enlarged screenshot of the area highlighted by the red bounding box in (a).

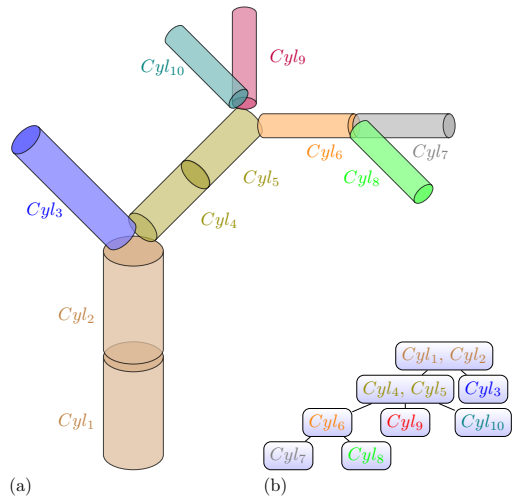

FIGURE 2

(a) An artificial QSM consisting of ten cylinders `Cyl`$_n$. Each cylinder consists of two 3d points `start` and `end` as well as the `Radius`. The cylinders between two neighboring branching junctions are combined to a list structure called segment. Each segment is colored differently. The cylinder list is always ordered from closest to the root to farthest away from the root.
(b) We can see the topological order information from the QSM in (a). The segments are stored in the nodes. The root node is the segment which contains the root cylinder. The child nodes are always ordered by the size of the `GrowthLength` of the child node's first cylinder.

The free tools have been tested by comparing QSM estimated `Volume` derived from TLS data versus destructive collected `Volume` field measurements (Hackenberg et al., 2021; Demol et al., 2022a).

1.5 | Technological outlook

Low cost photogrammetric sensors can serve as data collection tools when utilizing convolutional neural networks (Russell and Norvig, 2009) to compute depth maps from images. Those can be transformed to 3d point clouds which then could be utilized as input data for SimpleForest, TreeQSM, 3dForest or other tools. Constant break throughs (Chang and Chen, 2018; Tankovich et al., 2021; Lipson et al., 2021; Li et al., 2022) regarding accuracy of the derived photogrammetric clouds have been made by utilizing stereo vision cameras, which cost only about one tenth of the investment needed to purchase a TLS device.

The fact that even with every day photogrammetric sensors we can retrieve point cloud representations is of huge impact. The clouds can be calculated from multiple un-referenced images of various point of views inside a scenery (Kuhn et al., 2020; Zhang et al., 2020). Even monocular methods for producing highly accurate depth maps from single photographies exist (Alhashim and Wonka, 2018; Yuan et al., 2022).

And it is worth mentioning that future superior algorithms will produce more accurate depth images compared to nowadays algorithms on the same input data. We live in a time where we can create data bases with millions or even billions of tree measurements with every day technology. QSMs will be produced with free available tools on

photogrammetric clouds.

Neural networks implementing the so called fairness principle (Mehrabi et al., 2021) are starting to get frequently applied by artificial intelligence researchers. By theory training data containing different groups or populations requires equal distribution of data belonging to that groups. But reality has shown that training data often does not fit this requirement. The fairness approach is helpful to handle the under representation of groups in the training data and we consider this approach helpful to adapt to flaws in the sampling design. A national forest inventory for example has to face such sampling flaws cause it is impossible to collect for a rarely occurring tree species the same amount of data as for a dominant tree species.

2 | METHODS

First we define new tree describing parameters and then we will build with two of them two functions which can predict the radius of a cylinder by looking at the topological information of the cylinder. We will use both functions in `Radius` filters designed to improve QSM data.

2.1 | Tree describing parameters

We will get aware of limitations by reading a QSM in the traditional way only. Traditional parameters like the `Branch Order` (`BO`) can be extracted. But we also have the potential to extract new yet untested and undiscussed parameters.

2.1.1 | Branch Order

The `BO` is counted from the stem up to the tips.

2.1.2 | Reverse Branch Order

To define another meaningful order in the sense of diameter scaling we can read the inverse branch order from a tree.

Reverse Branch Order The `Reverse Branch Order` (`RBO`) of a cylinder is the maximum depth of the subtree of the segment's node. If we look at the real tree, the `RBO` denotes the maximal number of branching splits of the sub-branch growing out the segment.

The reverse branch order is depicted in the schematic QSM in figure 3 b).

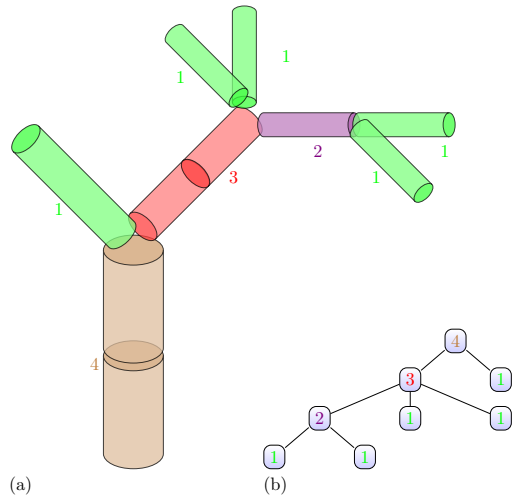

FIGURE 3

(a) The artificial QSM of figure 1 labeled with the `RBO` .
(b) We can see the topological order information from the QSM in (a) and each node has the `RBO` displayed.

2.1.3 | Reverse Branch Order Pipe Area

Reverse Branch Order Pipe Area We define the Reverse Branch Order Pipe Area (`RBOPA`): The WBE model considers that the branching architecture is self-similar (Brummer et al., 2017). In a self-similar branching architecture the `Radius` as well as the cross sectional area of a tip is constant. The `RBOPA` is a tree specific area unit. The expected cross sectional area of each tip of a tree equals `AreaOfTip` cm^2. `AreaOfTip` is later crossed out in our calculus so we do not have to compute it in the following. By following the pipe model theory (Shinozaki et al., 1964a) the `RBOPA` of a cylinder at any location inside the QSM equals the number of supported tips. Supported tip cylinders always have a recursively defined parent relation to the query cylinder.

We can see the `RBOPA` depicted in the schematic QSM visible in figure 4.

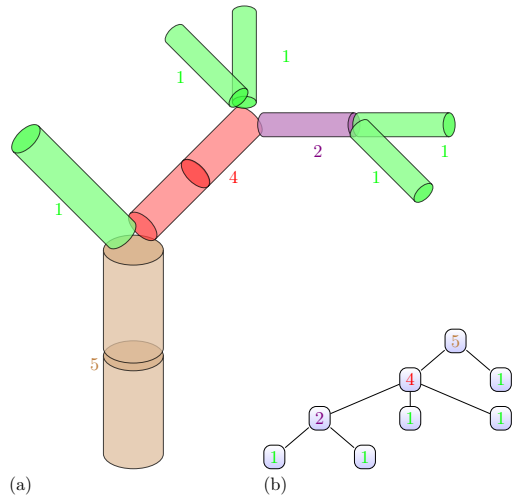

FIGURE 4

(a) The artificial QSM of figure 1 labeled with the `RBOPA` .
(b) We can see the topological order information from the QSM in (a) and each node has the `RBOPA` displayed.

By its definition the `RBOPA` is a proxy for the sapwood area. To derive the true sapwood area measured in metrical units we need to simply multiply `RBOPA`× `AreaOfTip`.

2.1.4 | Reverse Branch Order Pipe Radius

Earlier works have shown that small cylinders can represent the topology correctly, but their radius tends to be overestimated (Hackenberg et al., 2015b; Demol et al., 2022b). By having a radius independent proxy for the cross sectional area we can simply take its square-root to derive a proxy for the radius of a cylinder.

Reverse Branch Order Pipe Radius We define the Reverse Branch Order Pipe Radius (`RBOPR`) as the square root of the `RBOPA`.

2.1.5 | GrowthVolume

We defined in (Hackenberg et al., 2015a) the `GrowthVolume` of a cylinder recursively.

GrowthVolume The `GrowthVolume` of a cylinder is the cylinder's volume plus the `GrowthVolumes` of its children.

To get a better understanding of the `GrowthVolume` concept we use imagination and prune a real tree at exactly one branch or stem position of our choice in our mind. We will cut then a subtree/branch of our real tree and the `GrowthVolume` is the volume of this sub tree. The cylinder for which this `GrowthVolume` is the cylinder covering the imaginary pruning position, see figure 5.

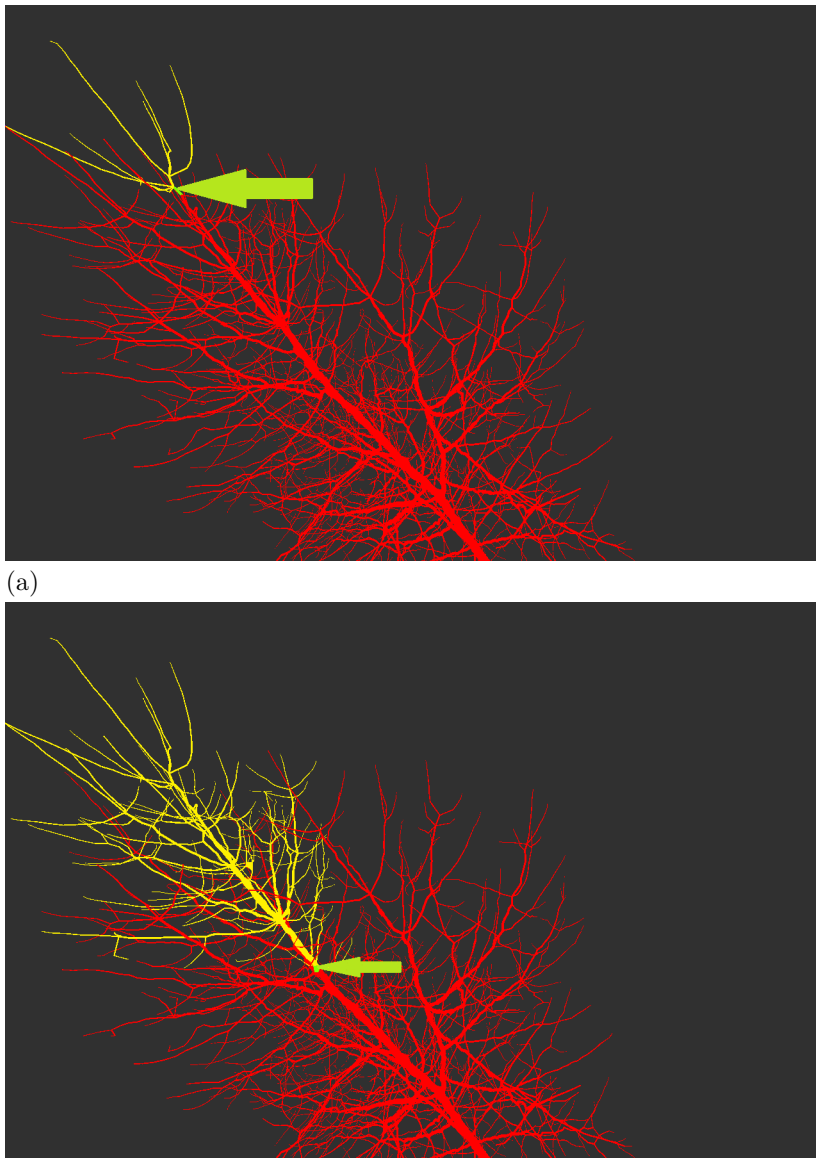

FIGURE 5

We see a QSM colored in three different colors to express visually the concept of recursive child definition for a cylinder. In green we see a query cylinder. Yellow are all cylinders which have a recursive child relation to that query cylinder. Red are all cylinders colored which do not fit the requirement. If we imagine pruning the real tree at the query position, the recursive child relation tree part is the subtree or branch we cut after pruning. In (a) the query cylinder is close to the tip and in (b) the query cylinder is placed in the center of the QSM. The root cylinder's recursive children are all cylinders of the QSM.

We used the `GrowthVolume` as a predictor for the radius in a radius correction filter (Hackenberg et al., 2015a), see equation 8.

$$radius = a \times GrowthVolume^{b} \tag{8}$$

Nevertheless this filter has a design flaw. Overestimated `Radii` of cylinders belonging to the `GrowthVolume` part affect their `Volumes` and therefore also the `GrowthVolume`. Our predictor is affected by the noisy attribute we want to get rid of and we will propose here later replacement for the `GrowthVolume` not having that design flaw.

2.1.6 | GrowthLength

We can substitute the volume in our previous definition to get a recursively defined length.

GrowthLength The `GrowthLength` of a cylinder is the cylinder's volume plus the `GrowthLength` of its children.

As the `GrowthLength` is not affected by radius prediction errors during cylinder fitting it is a robust ordering predicate, see figure 2. With other ordering predicates such as the `GrowthVolume` we encountered wrongly extracted stem cylinders. With a faultless ordering we can extract the stem by following the left path in the QSM structure depicted in the figure 2.

2.1.7 | ProxyVolume

As the `RBOPA` is a proxy for the area of active vessels which pass the cylinder we can also model a proxy for the volume occupied by vessels in a cylinder.

ProxyVolume The `ProxyVolume` of a cylinder is calculated by multiplying the `Length` with the `RBOPA` as shown in equation 9. By definition the `ProxyVolume` is not relying on correctly modeled `Radii`.

$$ProxyVolume = RBOPA \times length \tag{9}$$

2.1.8 | VesselVolume

We had defined the `GrowthVolume` of a cylinder in a recursive manner. We used the `GrowthVolume` in earlier works (Hackenberg et al., 2015a) as a predictor for a corrected radius of each cylinder utilizing a simple power function fit. In similar manner to the `GrowthVolume` we can define the `VesselVolume`, but utilizing instead of cylinders' `Volumes` their `ProxyVolumes`.

VesselVolume The `VesselVolume` of a cylinder is its `ProxyVolume` plus the `VesselVolume` of the cylinder's children.

2.2 | Comparison of parameters

In branch order one, not only the largest branch segment is included, but also medium sized branches and even epicormic shoots. Therefore the correlation between this branch order and the diameter of segments of a certain branch order is rather low, see figure 6 a).

We can see a stronger correlation for the `RBO` compared to the `BO` if we look into the scatter plots of `BO` vs `Radius` and `RBO` vs `Radius`.

There is a proxy potential with a linear pattern in figure 6 (c) on non log transformed input data.

In contrast to the `GrowthVolume` the `VesselVolume` is not affected by overestimated `Radii` and its correctness relies purely on correct topology. It shows a sharp curved pattern in 6 (d).

2.3 | QSM Filters

We are about to present two useful filters relying on the `Radius` prediction capabilities of the presented tree measures. No matter if linear or non linear fitting techniques are utilized it is a good behavior to prepare the QSM data. We want to detect cylinders with overestimated `Radii` and not use the measurements of those cylinders in the following fitting routines. As overfitting during the QSM generation is more likely to happen at the tip regions (Hackenberg et al., 2015b; Demol et al., 2022b), we can simply create one filter to get rid of overestimated cylinders by thresholding the `RBO`. For example Requesting the the `RBO` of valid cylinders has to be larger one removes all tip segments.

The remaining cylinders can then be piped through a statistical outlier filter based on the cylinder's distance to the aligned TLS sub-cloud.

2.3.1 | Linear RBOPR filter

The smaller the `RBOPR` the `Radius` residual is. So we might conclude to not have a homoscedastic, neither a heteroscedastic error. But we know from earlier works that the modeling error for tips is already caused by the input point data itself. Co-registration errors or the foot print size of the Laser already have a significant error impact (Demol et al., 2022b). As the true ground truth tree structure of tip regions is only reflected to some extend in the input clouds we conclude we cannot make an assumption on the underlying distribution of natural `Radius` variation.

We will build the `RBOPR` filter to correct overestimated `Radii` with equation 10.

$$radius = a \times RBOPR \tag{10}$$

We only correct `Radii` if they differ by more than a user selected percentage deviation threshold from their predicted `Radii`.

2.3.2 | Non linear VesselVolume filter

As with the `GrowthVolume` we can try to predict the radius from the `VesselVolume` by a simple non linear power fit as we see in figure 6 (d). So we will use equation 11 to correct cylinders `Radii` and will refer to as the `VesselVolume` filter. To get appropriate initial parameters required for non linear solvers we use the Huxley method on log transformed data (Huxley, 1924).

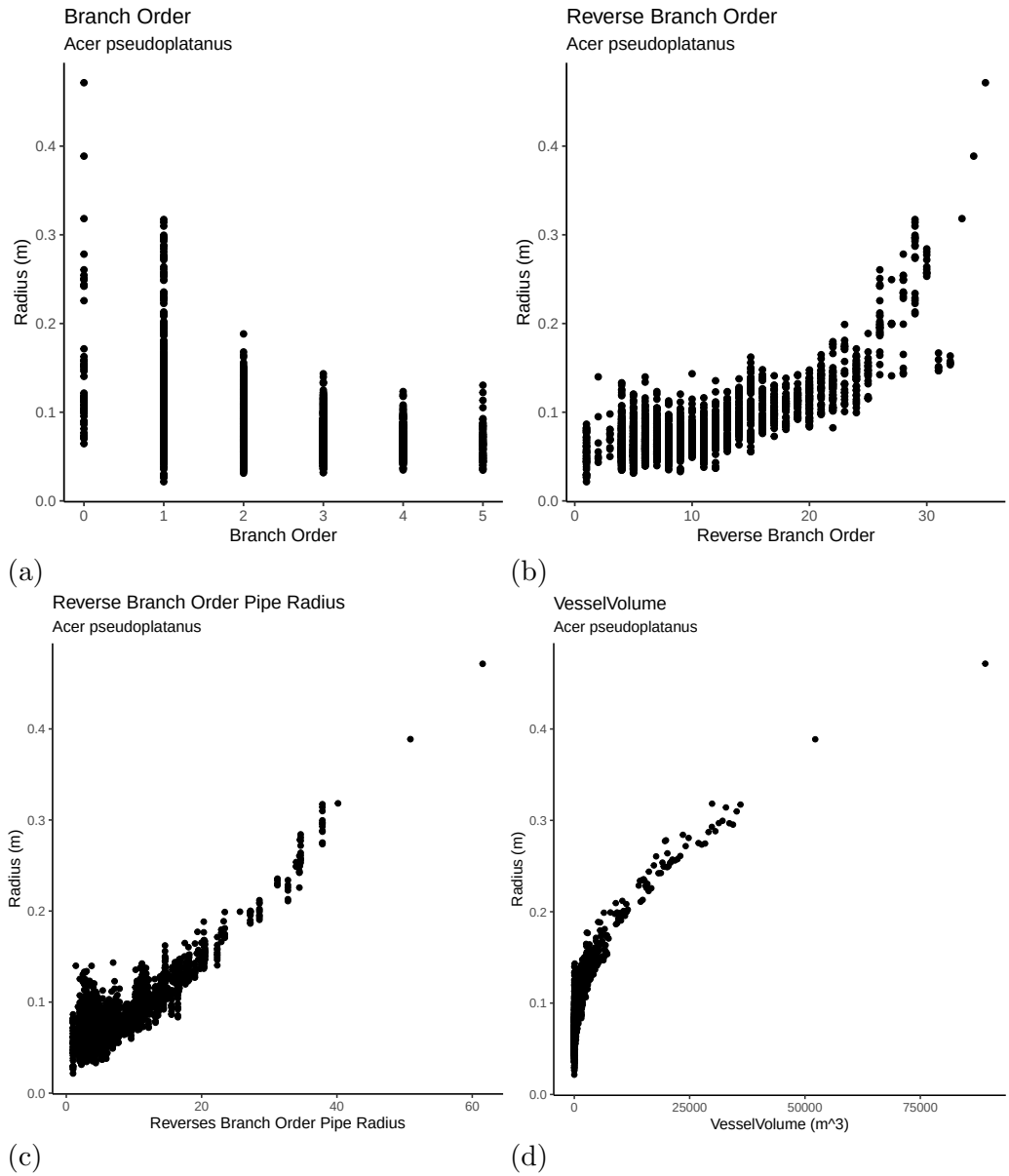

FIGURE 6

(a)

We see the correlation between the traditional `BO` and the `Radius` is not strong. Nevertheless the maximum value per branch order reveals a parabolic pattern.
(b) We see the correlation between the `RBO` and the `Radius` is stronger than the one depicted in (a). We see a noisy non linear pattern.
(c) When looking at the scatter plot of the `RBOPR` vs the `Radius` we can see a linear pattern, less noisy than the pattern in (b).
(d) A power function form non linear pattern is visible when we plot the `VesselVolume` vs the `Radius`. This pattern is the best in the sense that we barely see noise here.

$$radius = a \times VesselVolume^{b} \tag{11}$$

To be in agreement with the geometrical relation between a `Volume` and a `Length` we expect b close to the cube root $\frac{1}{3}$.

The solver can still fail, if too large residuals are contained in the fitting data. Non linear fitters are less robust as they can find false, local minima instead of global minima in the error distribution. To get robust against such failiures we recommend to first apply the Filter based on the RBOPR with a large deviation threshold. The linear correction will be applied to the cylinders with the largest errors, but a lot of unmodified cylinders are still usable to predict the `VesselVolume` power function parameters.

The allowed deviation between measured and predicted before we apply a `Radius` correction is user selected in same manner as in the `RBOPR` filter routine.

2.4 | Data

The author's of (Demol et al., 2021a) destructively harvested 65 individuals of the species *Fagus sylvatica*, *Larix decidua*, *Pinus sylvestris*, *Fraxinus excelsior*. From `AGB` measurements and density analysis `Volume` reference data was derived. Then the authors produced 65 QSMs with TreeQSM version 2.4.1 (Raumonen, 2022). For TreeQSM models a tapering filter (Calders et al., 2015) relying on a parabolic function to correct overestimated leaves was applied. Both TreeQSMs and cloud data was published at Zenodo (Demol et al., 2021b).

QSMs have been produced as well with SimpleForest v 5.3.1 (Hackenberg, 2021; Hackenberg et al., 2021). We applied the following pipeline on the input clouds:

1. apply a statistical outlier filter on the input clouds (Rusu and Cousins, 2011),
2. produce QSMs with the SphereFollowing method wrapped in an automated parameter search (Hackenberg et al., 2015a; Donati Sarti et al., 2022),
3. apply the `RBOPR` filter,
4. apply the `VesselVolume` filter.

3 | RESULTS

Results in this section have been produced with R-Software (R Core Team, 2022) and for the plots we used ggplot (Wickham, 2016).

3.1 | Comparing against the QSM state of the art

As we have destructively collected reference `Volume` data (Demol et al., 2021b) we can analyze the accuracy of QSM `Volume` predictions. In figure 7 we use SimpleForest QSMs which have been improved by either the linear `RBOPR` filter (a) or the non-linear `VesselVolume` filter (b). We plot as well the results produced with TreeQSM as published (Demol et al., 2021b) (c).

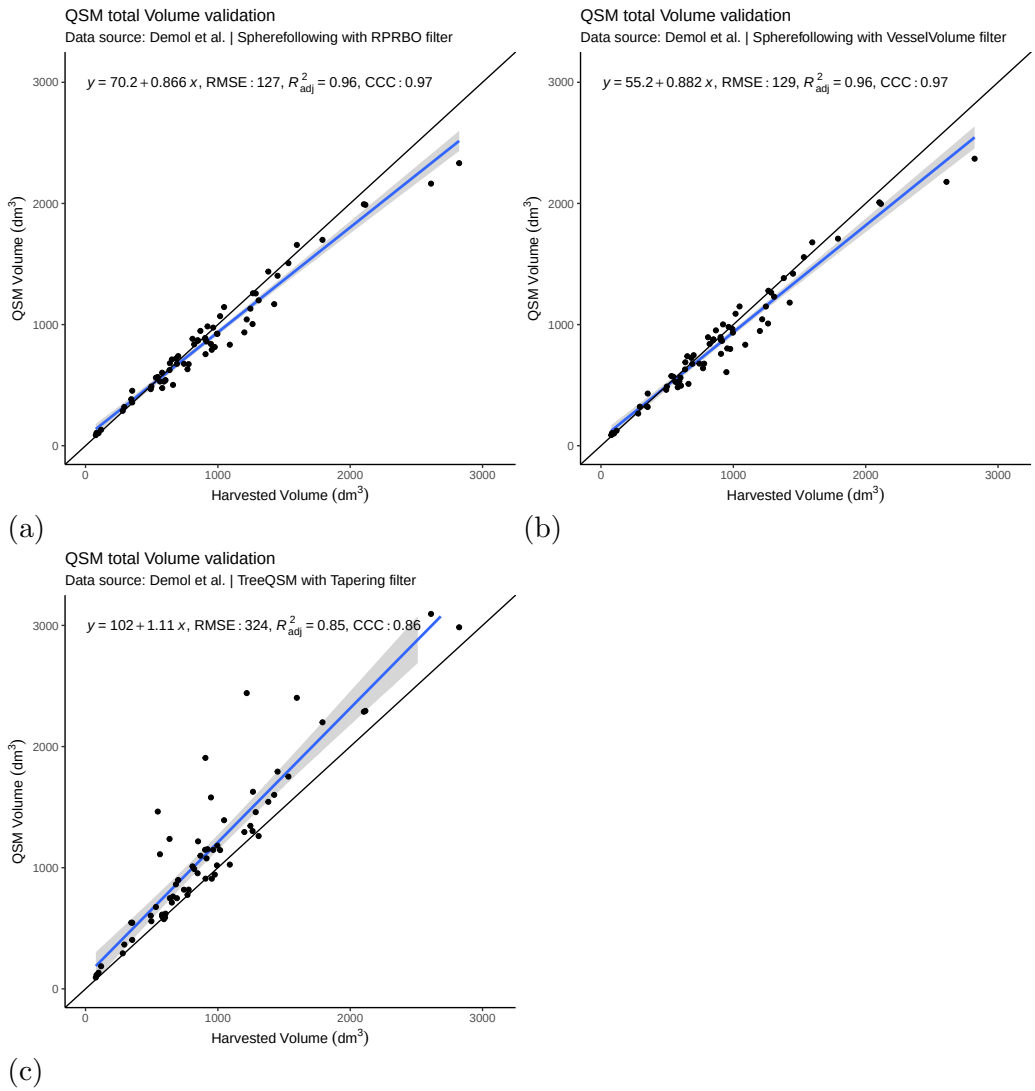

FIGURE 7

We use free accessible data (Demol et al., 2022a) .

(a) SimpleForest QSMs filtered with the `RBOPR` filter have their `volumes` compared to destructive ground truth measurements.
(b) Similar to (a), but this time the `VesselVolume` filter was applied to SimpleForest QSMs.
(c) We also show the scatter plot of QSMs stored in the data base. Those have been modeled with TreeQSM algorithm (Raumonen et al., 2013) and then filtered by the TreeQSM tapering method (Calders et al., 2015).

All results are written with their root mean squared error (RMSE), their $r^2_{adj.}$ and their Concordance Correlation Coefficient (CCC) into table 1.

TABLE 1 Numerical validation of QSM volume measures compared to harvested reference volume measures.

Software	RMSE (dm^3)	$r^2_{adj.}$	CCC
SimpleForest `VesselVolume`	129	0.96	0.97
SimpleForest `RBOPR`	127	0.96	0.97
TreeQSM `Tapering`	324	0.85	0.86

3.2 | Applying and adapting the Huxley protocol

We took the output of the `VesselVolume` filtered pooled QSM data and looked into the pooled data applying the Huxley protocol. We used as input only data of those cylinders, which did not have been modified by the filter. An unmodified cylinder means that the `Radius` is still the least squares fitted radius. For all trees we still had 13965 cylinders left and those are shown in figure 8. At first glance the untransformed data (a) looks quite diverse. While we can see species clustering also within species the tree individuals show unique patterns. The linear model on the log transformed data (b) shows already a species wise correlation quantified by $r^2_{adj.}$ ranging between 0.89 and 0.96. But if we normalize the `VesselVolume` and the `Radius` to scale for each tree between 0 and 1 a strong pattern is revealed in the not log transformed data (c). The $r^2_{adj.}$s of the species wise linear models range from 0.96 to 0.97 and the slopes of the fitted lines are quite similar in a range of 0.34 to 0.36 (d).

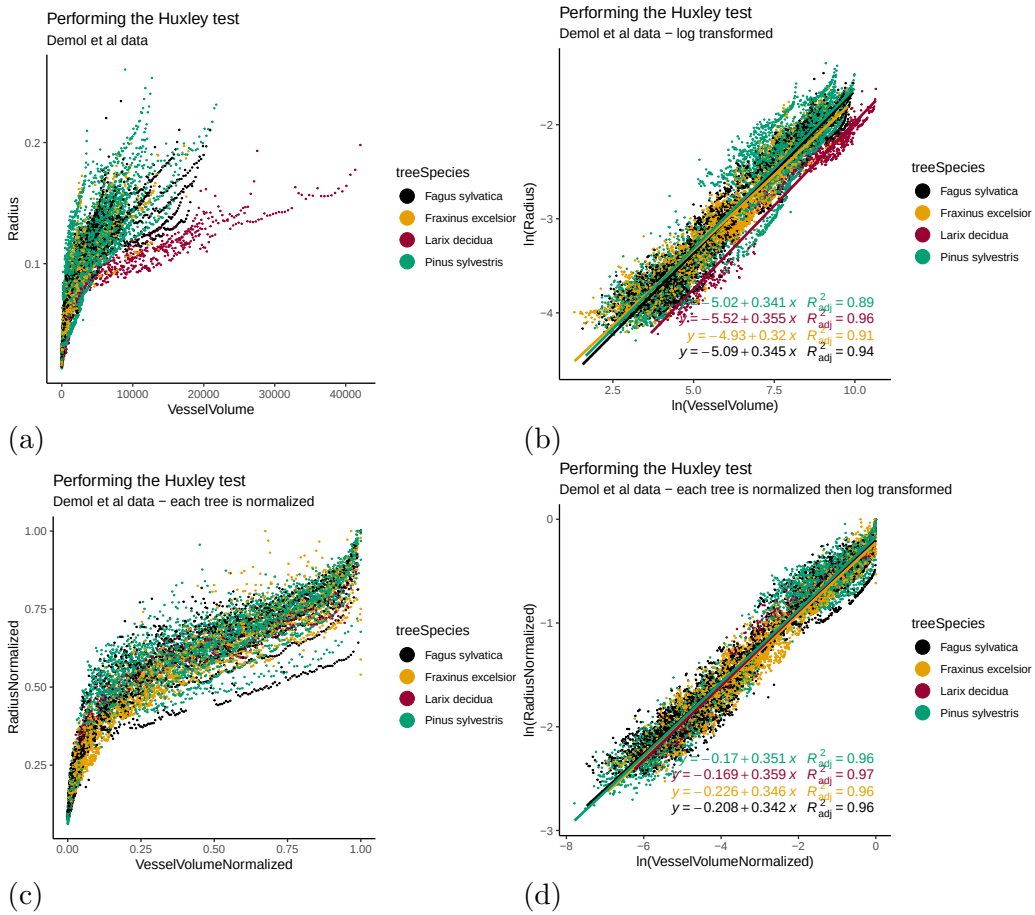

FIGURE 8

(a) The scatter plot of `Radius` vs `VesselVolume` of 13965 cylinders originated of SimpleForest QSMs produced with the data of Demol (Demol et al., 2022a).
(b) The scatter plot of the log transformed data of (a) with linear models fitted per species.
(c) The data of (a), but we normalized each QSM before pooling to have the `VesselVolume` and the `Radius` scale between 0 and 1.
(d) After a log transform of data in (c) we fit again linear models per species.

3.3 | Testing the WBE

Enquist published values of allometric exponential power coefficients for various tree parameter relations (Enquist, 2002). A few of them we can model with QSM data. Enquist uses as input variable `AGB` which we only approximate with the `GrowthVolume` in this work. We excluded here as well modified cylinders and plotted four allometric relations based evaluated on more than 10'000 measurements in figure 9. We pooled all species together and normalized all

parameters to scale between 0 and 1 for each tree.

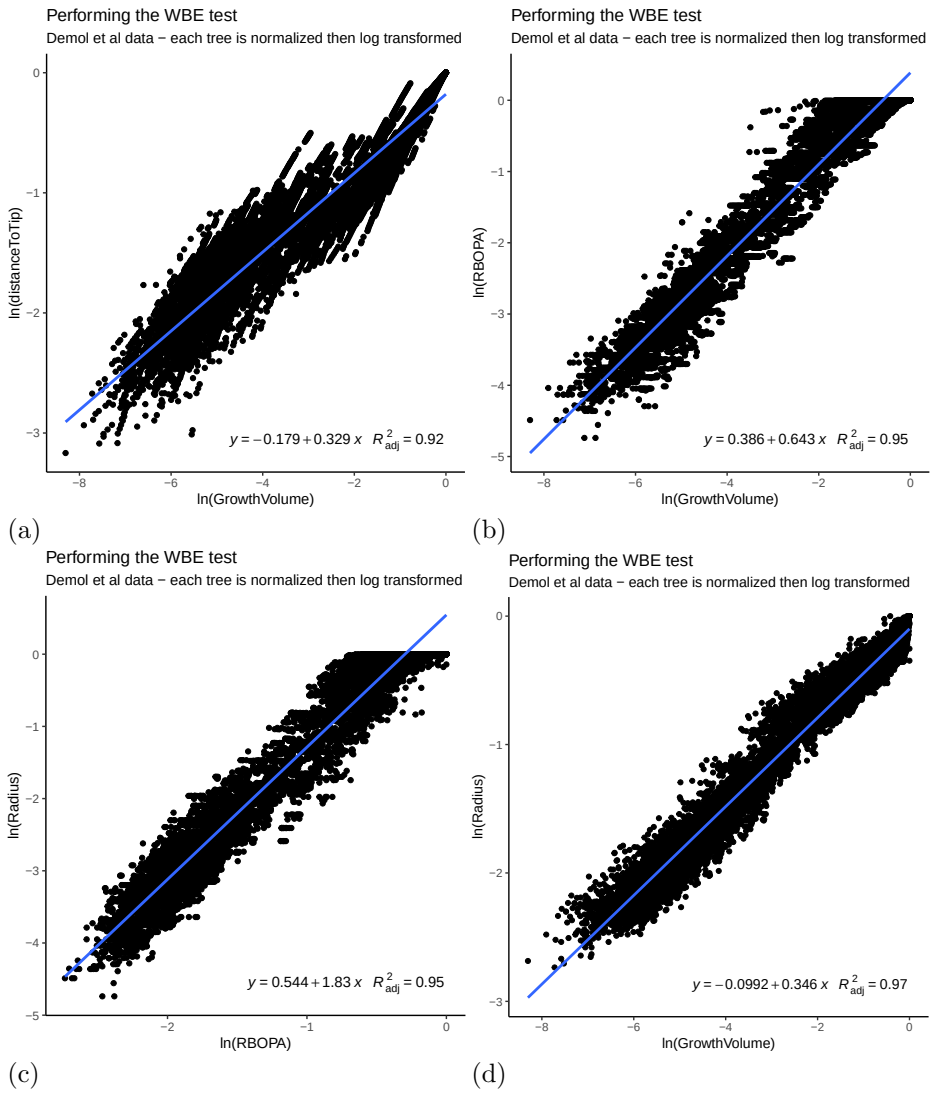

FIGURE 9

(a) The scatter plot of `GrowthVolume` vs `DistanceToTip` of 12352 cylinders on the log transformed domain.
(b) The scatter plot of `GrowthVolume` vs `RBOPA` of 12352 cylinders on the log transformed domain.
(c) The scatter plot of `RBOPA` vs `Radius` of 12352 cylinders on the log transformed domain.
(d) The scatter plot of `GrowthVolume` vs `Radius` of 12352 cylinders on the log transformed domain.

`PlantMass`, `NumberOfBranches`, `BranchLength` and `Radius` are part of the parameter set for which Enquist pre-

dicts the allometric scaling exponents. We compare our estimates with Enquist's in table 2 where we use:

1. `GrowthVolume` as a proxy for `PlantMass`,
2. `RBOPA` as a proxy for `NumberOfBranches`,
3. `DistanceToTip` as a proxy for `BranchLength`.

TABLE 2

Allometric relation	$r^2_{adj.}$	$b_{QSM-predicted}$	$b_{Enquist-predicted}$
$DistanceToTip - GrowthVolume$	0.92	0.33	0.25
$RBOPA - GrowthVolume$	0.95	0.64	0.75
$Radius - RBOPA$	0.95	1.83	2
$Radius - GrowthVolume$	0.97	0.35	0.38

3.4 | Presenting new allometric relations for future tree modeling theories

In figure 10 we show a four relations which cannot be modeled with parameters measured with traditional methods. We rely in all functions on either the `VesselVolume`, the `GrowthVolume` or the `GrowthLength`.

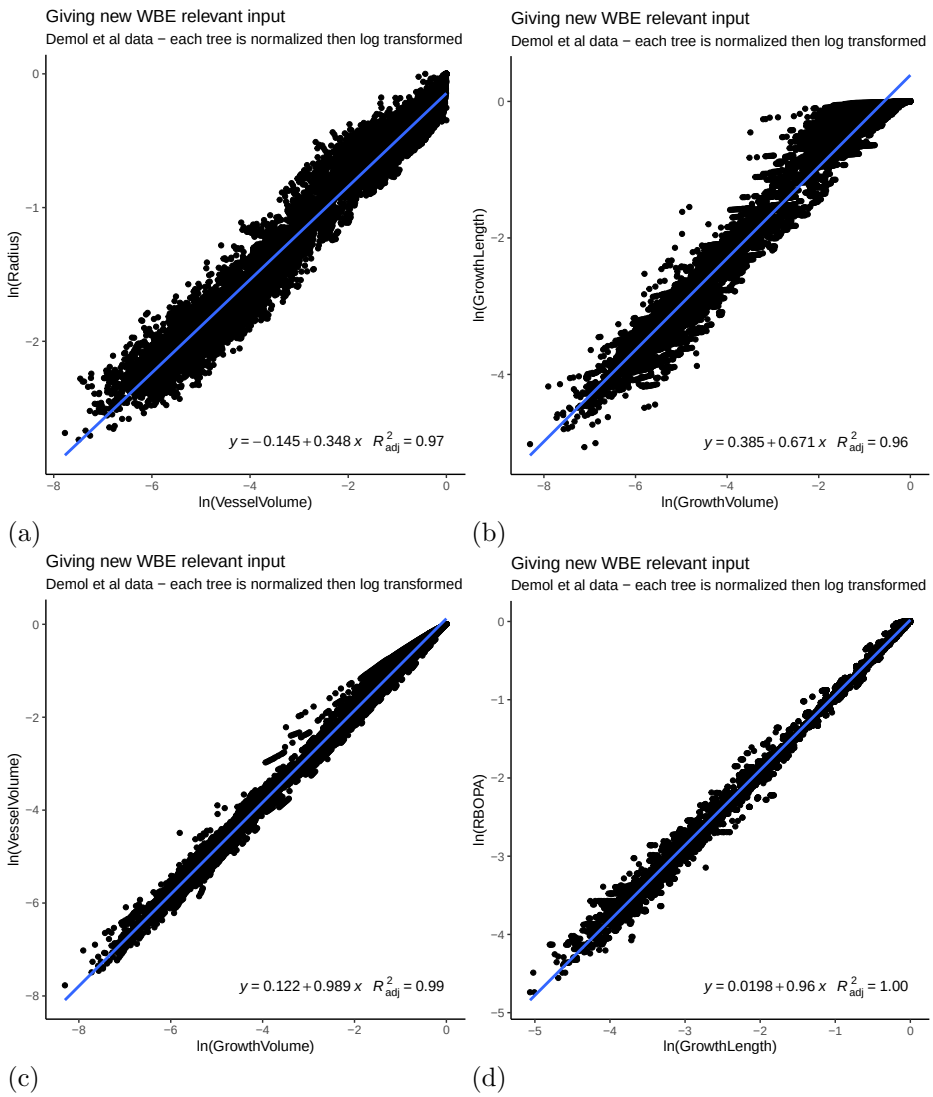

FIGURE 10

(a) The scatter plot of `VesselVolume` vs `Radius` of 12352 cylinders on the log transformed domain.
(b) The scatter plot of `GrowthVolume` vs `GrowthLength` of 12352 cylinders on the log transformed domain.
(c) The scatter plot of `GrowthVolume` vs `VesselVolume` of 12352 cylinders on the log transformed domain.
(d) The scatter plot of `GrowthLength` vs `RBOPA` of 12352 cylinders on the log transformed domain.

The results are written in table 3.

TABLE 3

Allometric relation	$r^2_{adj.}$	$b_{QSM-predicted}$
$Radius - VesselVolume$	0.97	0.35
$GrowthLength - GrowthVolume$	0.96	0.67
$VesselVolume - GrowthVolume$	0.99	0.99
$GrowthLength - RBOPA$	1.00	0.96

3.5 | Revealing additional details in un-pooled data

We see in figure 11 for a QSM build from a *Fraxinus excelsior* cloud that an inverted s-shaped function might be more appropriate compared to a simple power function. But as we also see the potential to split the data into two parts we prefer model each part with an individual power function. The red colored stem cylinder parameters are all cylinders with `BO` zero which start coordinate is lower than the `CrownBaseHeight`. $\mathtt{r}^2_{\mathtt{adj.}}$ numbers on the log transformed scale are 0.95 for the crown, but only 0.85 for the stem.

CrownBaseHeight The crown starts with the largest branch and we can detect the largest branch inside a QSM by looking for the cylinder which has the largest `GrowthLength` of all cylinders with a `BO` larger zero. The z-coordinate of that cylinder's start point is the `CrownBaseHeight`.

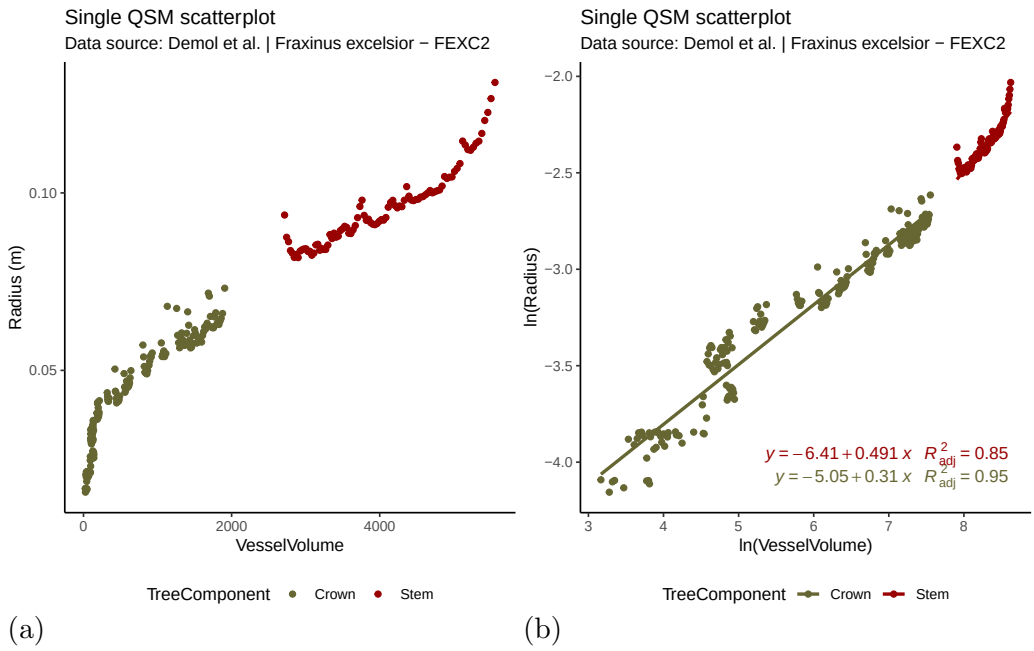

FIGURE 11

We see cylinder measurements of one QSM of a *Fraxinus excelsior* individual - data base name FEXC2. The QSM was filtered with the `VesselVolume` filter. All modified cylinders have been removed from the analysis. The green dots correspond to branch cylinders and the red to ones to stem cylinders.

(a) The whole curve can be described with a s-shaped temporal growth function or split into two data sets and fit two power functions separately for lower stem and crown respectively. Approaches to fit multiple lines into quasi-linear parts have been done already in the early years of allometric research (Huxley, 1924).

(b) In fact only the crown seems to follow a linear pattern, the nature of the stem points reveals a curvilinear pattern. The statement is undermined with $r^2_{adj.}$ values of 0.95 for crown, but only 0.85 for fitting a linear model into the stem points.

4 | DISCUSSION

4.1 | QSM Volume Accuracy

We imported here in our analysis results (Demol et al., 2021a,b) which have been produced with TreeQSM. The TreeQSM pipeline which was utilized by Demol et al. uses an algorithm which has been discussed in detail (Raumonen et al., 2013). To achieve an automated parameter search that algorithm was embedded into optimization techniques discussed in (Hackenberg et al., 2015a). The QSMs then were filtered with the tapering method (Calders et al., 2015).

Importing the same clouds we also produced SimpleForest QSMs relying on the same parameter optimization technique (Hackenberg et al., 2015a) but utilizing a different algorithm - the spherefollowing algorithm (Hackenberg

et al., 2014). The output QSMs have then been filtered with the here proposed allometric theory based filters. We fitted linear models into the ground truth `Volume` vs QSM `Volume` predictions, see figure 7 and table 1.

Our results produced data where the `RMSE` is 39 % of the TreeQSM error. The devation of the $r^2_{adj.}$ value from the best score 1.0 is for SimpleForest only 27 % of the TreeQSM derived deviation. For the `CCC` the deviation is only 21 % of the TreeQSM deviation.

To get more insight into the error we want to split up the total error into a measurement error ($error_{ref}$) of the destructively collected reference data, the error produced by the algorithm ($error_{alg}$) which is limited by the potential of the filter to reduce exactly this error ($potential_{fil}$), see equation 12.

$$error_{total} = error_{ref} + error_{alg} \times potential_{fil} \tag{12}$$

The $error_{ref}$ is the exact same for TreeQSM as well as SimpleForest results. Therefore we will purely focus in the following on $error_{alg}$ and $potential_{fil}$. With the data here used we only show that SimpleForest with one of the allometric scaling filters performs better than TreeQSM with the tapering filters. For splitting up the error further a more complex result matrix would have to be generated.

We conclude that the analyzed tree species can be modeled with the here presented allometric scaling theory based filters. Using our introduced allometric relations performes better than previously published QSM filtering methods (Calders et al., 2015; Hackenberg et al., 2015a).

We can further see an underestimation of the prediction by SimpleForest. Time series data recorded under temporal changing weather and climate conditions might open here a complete new field. In hot dry years we might observe underestimation as the sapwood volume which we use as a predictor is less than in humid and mild years.

4.2 | Pooling data of different trees

Huxley's work (Huxley, 1924) and follow up publications pool the data of multiple individuals. They use one parameter set per individual. The QSM filters though are based on measurements of one tree only. This is justifiable as QSMs can contain multiple thousand cylinders. Even after our proposed pre-filters to remove over-fitted cylinders enough measurements remain for both the linear and non-linear fit. In fact if we pool all cylinder of the 65 trees we receive more than 13'000 uncorrected cylinders from which we can read a multitude of parameters.

We want to test if we can apply the Huxley protocol to pooled data. We sub-devide our measurements per species and plot `Radius` vs `VesselVolume` in figure 8 (a). The plot reveals that individuals of *Larix decidua* have more `VesselVolume` increment per `Radius` increment than individuals of *Fagus sylvatica* have. At first glance the pooling of all trees seems difficult. Even more difficult as we can unambiguously detect individual tree patterns also within one species.

Still we look on the log transformed data (b). In the log transformed domain between and within species variation vanishes a bit. We can fit linear models per species with $r^2_{adj.}$ of 0.89, 0.96, 0.91 and 0.94. Acceptable $r^2_{adj.}$ values but the slope of the models range from 0.34 to 0.36. So the allometric exponents vary a bit and in exponential functions a variation of the exponent has a large impact on the predicted value.

If we normalize our input parameters to range between 0 and 1 by dividing with the maximum value of that parameter per QSM we cannot anymore easily detect tree individual patterns by observation (c).

This statement is undermined by a better $r^2_{adj.}$ ranging from 0.96 to 0.97 and also the slope variation decreased to 0.34 up to 0.35 (d).

The slope is parameter b of equation 11. Our calculated values are in agreement with the previously made assumption that b needs to be close to $\frac{1}{3}$. We predict a length from a volume with the cube root.

We conclude that it makes sense to build more complex allometric functions with categorical variables (Packard, 2019), but for the remaining analysis in this work we also found out that normalization is a technique which helps making data of different tree‘s or different species better comparable.

4.3 | How valuable is the WBE model

By comparison with reference data we found out that our filtered QSMs are a representation for the ground truth trees. As not all QSM cylinders are Radius filtered and we never modify the topological order in our QSMs by those filters we can collect 13’000 measurements which are derived from our algorithm relying on Gauss Newton cylinder fits (Hackenberg et al., 2014). We also found out that by normalization we can pool all those cylinders. We want to use this data to test exemplarily part of the tree modeling theories we reviewed in our introduction.

Some exponents of allometric relations have their allometric parameter published (Enquist, 2002). We compare our empirical predictions against theirs. Using the GrowthVolume as a proxy for the AGB we can for example build the so important Diameter vs AGB relation. Enquist predicts here an exponential factor of 0.38 and our predicted value for the Radius vs GrowthVolume relation is with 0.35 quite close. This is unexpected as our AGB proxy ignores all density variation influences and purely relies on the summed up cylinder Volumes. The Radius vs RBOPA relation which to some extend corresponds to the Diameter vs NumberOfBranches relation deviates only less than ten percent from the Enquist prediction. The Branchlength vs AGB relation is represented by DistanceToTip vs GrowthVolume relation. Here the linear model performs worse than the other models. A reason to question this relation on theoretical ground is that we model the relation of a linear path length of the branching structure with a recursive measure which includes side branches. In other words, in that relation predictor and predicted do not represent the same parts of the tree. Our predicted 0.33 is far away from Enquist 0.25. RBOPA scales with the GrowthVolume with an exponential factor of 0.64. Enquist predicts here 0.75.

4.4 | Discussing new parameters and their allometric relations

By using scan data of 65 trees we derive 13’000 measurements, ~ 100 times more than research relying on traditional non digital data used (Shinozaki et al., 1964a; Packard, 2019). Also here introduced parameters such as the RBOPA, GrowthLength or VesselVolume can be extracted from QSMs. We show four relations in figure 10 and table 3. The first relation between Radius and VesselVolume is the one the SimpleTree filter uses. But now we model pooled data of all trees. The $r^2_{adj.}$ is 0.97. Slightly less accurate is the second model for the GrowthLength vs GrowthVolume relation which has an $r^2_{adj.}$ of 0.96. The performance of scaling between VesselVolume and GrowthVolume reaches a $r^2_{adj.}$ of 0.99. This relation is already stronger than all the ones we analyzed before. And if we look on the parameters we see that the exponential parameter is close to 1 with 0.99. So we expect to have a linear relation between the area of active pipes and the total area of active and unactive pipes at any point in the tree. RBOPA and GrowthLength perform similarly well.

5 | CONCLUSIONS

5.1 | Impact on QSM usage

We recommend the usage of one of the two the here presented filtering protocols when working with QSMs. To our knowledge no national forest inventory decided to use QSMs to build `Volume` functions from it up to date. This work provides a significant boost for the `Volume` prediction capabilities of QSMs so we recommend a reevaluation of QSM usage potentials.

Generalization of the results should be handled with care. We analyzed here data recorded in leave-off conditions with multiple scans with state of the art equipment and protocols (Demol et al., 2021a). Only if similar scanning conditions are faced, the accuracy of the results can be expected of the same order as discussed.

Prooning campaigns which are designed to influence a tree's growth pattern to produce the maximal amount of merchantable wood might result in tree individuals following growth patterns not fullfilling of the here applied Huxley protocol (Huxley, 1924). How well this work performs on either conifers or large evergreen trees needs to be analyzed as well.

5.2 | Impact on forest ecology theories

The `RBOPA` we interpreted as a proxy for the area of sapwood at any given point in the tree. Of course we could also think of multiplying the `RBOPA` with the expected number of leaves on a new growth unit and derive the total number of leaves. So the `RBOPA` can be seen as a proxy for the area leave index as well.

With open QSM data bases tree modelers have from now on a much more convenient way to collect data.

5.3 | Future Work

We first want rework the preprinted SimpleForest software paper to provide an up to date reference for the here used free software tool (Hackenberg et al., 2021).

We also identified the need for a data paper about an open data-base-system of. Various data sets have already been made accessible (Hackenberg et al., 2015b; de Tanago et al., 2018; Demol et al., 2021a) and we want to combine all small data bases to a larger one backuped by a manuscript. We hereby would like to convince more data owners to share their data. Instead of 65 trees future analysis can be run on few hundred of tree clouds with harvested volume data.

We like to envisage a collaborative paper with TreeQSM and 3dForest personnel. As soon as the work on the data base paper is done we could run all three softwares unfiltered and combine each result with one existing filter technique.

5.3.1 | Improvement of filters

In fact we skipped a lot of potential analysis with this data. We sticked as much as possible to an 100 year old protocol (Huxley, 1924). But we also gave an overview over the protocol performed in (Packard, 2019). Future work should test different error terms and change the power function in various manners itself. Introducing catagorical variables such as the species category is possible as well. In figure 11 we reveal that the stem should be excluded from the filters. We still recommend also to use TLS data to build traditional stem taper functions.

acknowledgements

We would like to acknowledge Matthias Disney for providing the SimpleForest development with constructive feedback over the last decade via emails and manuscript reviews.

conflict of interest

The authors declare no conflict of interest.

Supporting Information

We use for the computation in addition to the mentioned data the persistent SimpleForest release v5.3.1 (Hackenberg, 2021).

The windows executable can be used to produce the data stored in our manuscript repository `https://gitlab.com/SimpleForest/allometricscalingpaper`.

We uploaded the needed Computree SimpleForest scripts as well as the R-statistic scripts to produce the results plots in that repository in addition to the QSM data.

references

Alhashim, I. and Wonka, P. (2018) High quality monocular depth estimation via transfer learning. *arXiv preprint arXiv:1812.11941*.

Anderson, D. and Burnham, K. (2004) Model selection and multi-model inference. *Second. NY: Springer-Verlag*, **63**, 10.

Anderson, D. R. (2008) *Model based inference in the life sciences: a primer on evidence*, vol. 31. Springer.

Bainbridge, J. (1969) Miscalculation? *Bioscience*, **19**, 770–770.

Banavar, J. R., Maritan, A. and Rinaldo, A. (1999) Size and form in efficient transportation networks. *Nature*, **399**, 130–132.

Brummer, A. B., Savage, V. M. and Enquist, B. J. (2017) A general model for metabolic scaling in self-similar asymmetric networks. *PLOS Computational Biology*, **13**, 1–25. URL: `https://doi.org/10.1371/journal.pcbi.1005394`.

Calder, W. A. (1984) *Size, function, and life history*. Harvard University Press, Cambridge.

Calders, K., Newnham, G., Burt, A., Murphy, S., Raumonen, P., Herold, M., Culvenor, D., Avitabile, V., Disney, M., Armston, J. and Kaasalainen, M. (2015) Nondestructive estimates of above-ground biomass using terrestrial laser scanning. *Methods in Ecology and Evolution*, **6**, 198–208. URL: `http://doi.wiley.com/10.1111/2041-210X.12301`.

Calders, K., Origo, N., Burt, A., Disney, M., Nightingale, J., Raumonen, P., Åkerblom, M., Malhi, Y. and Lewis, P. (2018) Realistic forest stand reconstruction from terrestrial lidar for radiative transfer modelling. *Remote Sensing*, **10**.

Chang, J. and Chen, Y. (2018) Pyramid stereo matching network. *CoRR*, **abs/1803.08669**. URL: `http://arxiv.org/abs/1803.08669`.

Côté, J.-F., Fournier, R. A. and Egli, R. (2011) An architectural model of trees to estimate forest structural attributes using terrestrial LiDAR. *Environment Modelling Software*, **26**, 761–777.

Demol, M., Calders, K., Krishna Moorthy, S. M., Van den Bulcke, J., Verbeeck, H. and Gielen, B. (2021a) Consequences of vertical basic wood density variation on the estimation of aboveground biomass with terrestrial laser scanning. *Trees*, **35**, 671–684.

Demol, M., Gielen, B. and Verbeeck, H. (2021b) QSMs, point cloud and harvest data from a destructive forest biomass experiment in Belgium using terrestrial laser scanning. URL: https://doi.org/10.5281/zenodo.4557401.

Demol, M., Verbeeck, H., Gielen, B., Armston, J., Burt, A., Disney, M., Duncanson, L., Hackenberg, J., Kükenbrink, D., Lau, A., Ploton, P., Sewdien, A., Stovall, A., Takoudjou, S. M., Volkova, L., Weston, C., Wortel, V. and Calders, K. (2022a) Estimating forest above-ground biomass with terrestrial laser scanning: Current status and future directions. *Methods in Ecology and Evolution*, **00**.

Demol, M., Wilkes, P., Raumonen, P., Moorthy, S. M., Calders, K., Gielen, B. and Verbeeck, H. (2022b) Volumetric overestimation of small branches in 3D reconstructions of Fraxinus excelsior. *Silva Fennica*, **56**, 1–26.

Disney, M. I., Boni Vicari, M., Burt, A., Calders, K., Lewis, S. L., Raumonen, P. and Wilkes, P. (2018) Weighing trees with lasers: advances, challenges and opportunities. *Interface Focus*, **8**.

Donati Sarti, G., Busa, M., Garnero, G., Magnani, A. and Rossato, I. (2022) An open-source approach to modelling and analysing a tree detected with a mobile laser scanner. In *Italian Conference on Geomatics and Geospatial Technologies*, 275–286. Springer.

Enquist, B. J. (2002) Universal scaling in tree and vascular plant allometry: toward a general quantitative theory linking plant form and function from cells to ecosystems. *Tree physiology*, **22**, 1045–1064.

Enquist, B. J., West, G. B. and Brown, J. H. (2009) Extensions and evaluations of a general quantitative theory of forest structure and dynamics. *Proc. Natl. Acad. Sci. U. S. A.*, **106**, 7046–7051.

Glass, N. R. (1969) Discussion of Calculation of Power Function with Special Reference to Respiratory Metabolism in Fish. *Journal of the Fisheries Research Board of Canada*, **26**, 2643–2650. URL: https://doi.org/10.1139/f69-256.

Hackenberg, J. (2021) SimpleForest Source Code and Documentation - v5.3.1. URL: https://doi.org/10.5281/zenodo.5138255.

Hackenberg, J., Calders, K., Demol, M., Raumonen, P., Piboule, A. and Disney, M. (2021) SimpleForest - a comprehensive tool for 3d reconstruction of trees from forest plot point clouds. *bioRxiv*. URL: https://www.biorxiv.org/content/early/2021/07/30/2021.07.29.454344.

Hackenberg, J., Morhart, C., Sheppard, J., Spiecker, H. and Disney, M. (2014) Highly accurate tree models derived from terrestrial laser scan data: A method description. *Forests*, **5**, 1069–1105.

Hackenberg, J., Spiecker, H., Calders, K., Disney, M. and Raumonen, P. (2015a) Simpletree — an efficient open source tool to build tree models from tls clouds. *Forests*, **6**, 4245–4294.

Hackenberg, J., Wassenberg, M., Spiecker, H. and Sun, D. (2015b) Non destructive method for biomass prediction combining tls derived tree volume and wood density. *Forests*, **6**, 1274–1300. URL: https://www.mdpi.com/1999-4907/6/4/1274.

Hafley, W. L. (1969) Calculation and Miscalculation of the Allometric Equation Reconsidered. *BioScience*, **19**, 974–983. URL: https://doi.org/10.2307/1294972.

Henry, M., Bombelli, A., Trotta, C., Alessandrini, A., Birigazzi, L., Sola, G., Vieilledent, G., Santenoise, P., Longuetaud, F., Valentini, R., Picard, N. and Saint-André, L. (2013) Globallometree: international platform for tree allometric equations to support volume, biomass and carbon assessment. *iForest - Biogeosciences and Forestry*, 326–330. URL: http://www.sisef.it/iforest/contents/?id=ifor0901-006.

Huxley, J. S. (1924) Constant differential growth-ratios and their significance. *Nature*, **114**, 895–896.

Kuhn, A., Sormann, C., Rossi, M., Erdler, O. and Fraundorfer, F. (2020) Deepc-mvs: Deep confidence prediction for multi-view stereo reconstruction. In *2020 International Conference on 3D Vision (3DV)*, 404–413. IEEE.

van Laar, A. and Akça, A. (2007) *Forest Mensuration*. Managing Forest Ecosystems. Springer Netherlands. URL: https://books.google.de/books?id=ybjdxL2lHOQC.

Lasiewski, R. C. (1969) Prefers Logarithmic Plotting. *BioScience*, **19**, 673–673. URL: https://doi.org/10.2307/1294889.

Lasiewski, R. C. and Dawson, W. R. (1969) Calculation and Miscalculation of the Equations Relating Avian Standard Metabolism to Body Weight. *The Condor*, **71**, 335–336. URL: https://doi.org/10.2307/1366309.

Lau Alvaro, Bentley Lisa Patrick, M. C. S. A. B. H. R. P. M. Y. J. T. H. M. (2018) Quantifying branch architecture of tropical trees using terrestrial LiDAR and 3D modelling.

Lehnebach, R., Beyer, R., Letort, V. and Heuret, P. (2018) The pipe model theory half a century on: a review. *Annals of botany*, **121**, 773–795.

Li, J., Wang, P., Xiong, P., Cai, T., Yan, Z., Yang, L., Liu, J., Fan, H. and Liu, S. (2022) Practical stereo matching via cascaded recurrent network with adaptive correlation. arXiv. URL: https://arxiv.org/abs/2203.11483.

Lipson, L., Teed, Z. and Deng, J. (2021) Raft-stereo: Multilevel recurrent field transforms for stereo matching. arXiv. URL: https://arxiv.org/abs/2109.07547.

Manaster B. J., M. S. (1975) Techniques for estimating allometric equations. *Journal of morphology*. URL: https://doi.org/10.1002/jmor.1051470305.

Markku, Å., Raumonen, P., Kaasalainen, M. and Casella, E. (2015) Analysis of geometric primitives in quantitative structure models of tree stems. *Remote Sensing*, **7**, 4581–4603. URL: https://www.mdpi.com/2072-4292/7/4/4581.

Medawar, P. B. (1950) Transformation of shape. *Proceedings of the Royal Society - Biological Sciences*.

Mehrabi, N., Morstatter, F., Saxena, N., Lerman, K. and Galstyan, A. (2021) A survey on bias and fairness in machine learning. *ACM Comput. Surv.*, **54**. URL: https://doi.org/10.1145/3457607.

Niklas, K. J. (2004) Plant allometry: is there a grand unifying theory? *Biological reviews*, **79**, 871–889.

Othmani, A., Lew Yan Voon, L. F., Stolz, C. and Piboule, A. (2013) Single tree species classification from Terrestrial Laser Scanning data for forest inventory. *Pattern Recognition Letters*, **34**, 2144–2150. URL: http://www.sciencedirect.com/science/article/pii/S0167865513002997.

Packard, G. (2019) Julian huxley and the quantification of relative growth. *Zoomorphology*, **139**, 131–140.

Peters, R. H. and Peters, R. H. (1983) *The ecological implications of body size*. Harvard University Press, Cambridge.

Pressler, M. R. and Pressler, M. (1865) gesetz der stammbildung und dessen forstwirthschaftliche bedeutung insbesondere für den waldbau höchsten reinertrago.

R Core Team (2022) *R: A Language and Environment for Statistical Computing*. R Foundation for Statistical Computing, Vienna, Austria. URL: https://www.R-project.org/.

Raumonen, P. (2022) TreeQSM code repository. https://github.com/InverseTampere/TreeQSM. [Online; accessed 16-July-2022].

Raumonen, P., Casella, E., Calders, K., Murphy, S., Åkerblom, M. and Kaasalainen, M. (2015) Massive-scale tree modelling from tls data. *ISPRS Annals of the Photogrammetry, Remote Sensing and Spatial Information Sciences*, **II-3/W4**, 189–196.

Raumonen, P., Kaasalainen, M., Akerblom, M., Kaasalainen, S., Kaartinen, H., Vastaranta, M., Holopainen, M., Disney, M. and Lewis, P. (2013) Fast automatic precision tree models from terrestrial laser scanner data. *Remote Sensing*, **5**, 491–520.

Richter, J. P. et al. (1970) *The notebooks of Leonardo da Vinci*, vol. 2. Courier Corporation.

Russell, S. and Norvig, P. (2009) Artificial intelligence: a modern approach.

Rusu, R. B. and Cousins, S. (2011) 3D is here: Point Cloud Library (PCL).

Sartori, A. F. and Ball, A. D. (2009) Morphology and postlarval development of the ligament of Thracia phaseolina (Bivalvia: Thraciidae), with a discussion of model choice in allometric studies. *Journal of Molluscan Studies*, **75**, 295–304. URL: https://doi.org/10.1093/mollus/eyp029.

Schmidt-Nielsen, K. (1984) *Scaling: why is animal size so important?* Cambridge University Press, Cambridge.

Shinozaki, K., Yoda, K., Hozumi, K. and Kira, T. (1964a) A quantitative analysis of plant form-the pipe model theory: Ii. further evidence of the theory and its application in forest ecology. *Japanese journal of ecology*, **14**, 133–139.

— (1964b) A quantitative analysis of plant form – the pipe model theory. i. basic analyses. *Japanese journal of ecology*, **14**, 97–105.

de Tanago, J., Lau, A., Bartholomeus, H., Herold, M., Avitabile, V., Raumonen, P., Martius, C., Goodman, R. C., Disney, M., Manuri, S., Burt, A. and Calders, K. (2018) Estimation of above-ground biomass of large tropical trees with terrestrial LiDAR. *Methods Ecol. Evol.*, **9**, 223–234.

Tankovich, V., Hane, C., Zhang, Y., Kowdle, A., Fanello, S. and Bouaziz, S. (2021) Hitnet: Hierarchical iterative tile refinement network for real-time stereo matching. In *Proceedings of the IEEE/CVF Conference on Computer Vision and Pattern Recognition*, 14362–14372.

Trochta, J., Krůček, M., Vrška, T. and Král, K. (2017) 3d forest: An application for descriptions of three-dimensional forest structures using terrestrial lidar. *PLOS ONE*, **12**, 1–17. URL: https://doi.org/10.1371/journal.pone.0176871.

Weibel, E. R. (2002) The pitfalls of power laws. *Nature*, **417**, 131–132.

West, G. B., Brown, J. H. and Enquist, B. J. (1997) A general model for the origin of allometric scaling laws in biology. *Science*, **276**, 122–126.

— (1999) The fourth dimension of life: fractal geometry and allometric scaling of organisms. *science*, **284**, 1677–1679.

— (2000) The origin of universal scaling laws in biology. *Scaling in biology*, 87–112.

West, G. B., Enquist, B. J. and Brown, J. H. (2009) A general quantitative theory of forest structure and dynamics. *Proceedings of the National Academy of Sciences*, **106**, 7040–7045. URL: https://www.pnas.org/doi/abs/10.1073/pnas.0812294106.

Wickham, H. (2016) *ggplot2: Elegant Graphics for Data Analysis*. Springer-Verlag New York. URL: https://ggplot2.tidyverse.org.

Xu, H., Gossett, N. and Chen, B. (2007) Knowledge and heuristic-based modeling of laser-scanned trees. *ACM Transactions on Graphics*, **26**, 19–es.

Ye, N., van Leeuwen, L. and Nyktas, P. (2019) Analysing the potential of UAV point cloud as input in quantitative structure modelling for assessment of woody biomass of single trees. *International Journal of Applied Earth Observation and Geoinformation*, **81**, 47–57. URL: https://www.sciencedirect.com/science/article/pii/S030324341831225X.

Yuan, W., Gu, X., Dai, Z., Zhu, S. and Tan, P. (2022) New crfs: Neural window fully-connected crfs for monocular depth estimation. *arXiv preprint arXiv:2203.01502*.

Zar, J. H. (1968) Calculation and Miscalculation of the Allometric Equation as a Model in Biological Data. *BioScience*, **18**, 1118–1120. URL: https://doi.org/10.2307/1294589.

Zhang, J., Yao, Y., Li, S., Luo, Z. and Fang, T. (2020) Visibility-aware multi-view stereo network. arXiv. URL: https://arxiv.org/abs/2008.07928.

Zianis, D., Muukkonen, P., Mäkipää, R. and Mencuccini, M. (2005) *Biomass and stem volume equations for tree species in Europe*. FI.

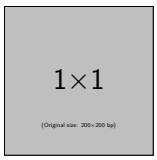

A. One Please check with the journal's author guidelines whether author biographies are required. They are usually only included for review-type articles, and typically require photos and brief biographies (up to 75 words) for each author.

GRAPHICAL ABSTRACT

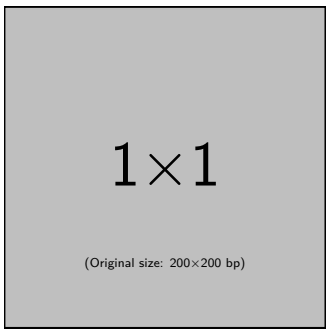

Please check the journal's author guildines for whether a graphical abstract, key points, new findings, or other items are required for display in the Table of Contents.